



# Bio-derived polyurethanes obtained by non-isocyanate route using polyol-based bis(cyclic carbonate)s—studies on thermal decomposition behavior

Paulina Parcheta-Szwindowska<sup>1</sup> · Kamila Rohde<sup>1</sup> · Janusz Datta<sup>1</sup>

Received: 16 February 2022 / Accepted: 29 September 2022  
© The Author(s) 2022

## Abstract

Non-isocyanate polyurethanes (NIPUs) constitute one of the most prospective groups of eco-friendly materials based on their phosgene-free synthesis pathway. Moreover, one of the steps of their obtaining includes the use of carbon dioxide (CO<sub>2</sub>), which allows for the promotion of the development of carbon dioxide capture and storage technologies. In this work, non-isocyanate polyurethanes were obtained via three-step synthesis pathway with the use of epichlorohydrin. In the I step, the addition reaction of epichlorohydrin with polyhydric alcohols was conducted for diglycidyl ethers obtaining. In the II step carbon dioxide reacted with diglycidyl ethers to obtain five-membered bis (cyclic carbonate)s in the cycloaddition reaction. Then, one-pot polyaddition reaction between bis (cyclic carbonate) and dimerized fatty acids-based diamine allowed for non-isocyanate polyurethanes (NIPU)s preparation. Three bio-based materials (two semi-products and one bio-NIPU) and three petrochemical-based materials (two semi-products and one NIPU) were obtained. The selected properties of the products of each step of NIPUs preparation were compared. Fourier transform infrared spectroscopy FTIR and proton nuclear magnetic resonance <sup>1</sup>H NMR measurements allowed to verify the chemical structure of all obtained products. The average molecular masses of the semi-products were measured with the use of size exclusion chromatography SEC. Moreover, thermal stability and thermal degradation kinetics were determined based on thermogravimetric analysis TGA. The results confirmed that the activation energy of thermal decomposition was lower for semi-products and NIPUs prepared with the use of petrochemical-based epichlorohydrin than for their bio-based counterparts.

**Keywords** Cycloaddition · Non-isocyanate polyurethane · Thermal decomposition · Carbon capture · Bis(cyclic carbonate) · Thermal degradation kinetics

## Introduction

Over the last half-century, it is very significant to replace hazardous chemicals and problematic reaction conditions with a more environmentally friendly solution [1]. Apart from the traditional method of polyurethane synthesis (with the use of diisocyanates), these materials can be obtained by isocyanate- and phosgene-free routes. The greatest potential represents polyaddition of bis(cyclic carbonate)s and di- or polyamines leading to non-isocyanate polyurethanes

(NIPUs) [2]. The advantages include the possibility of using bio-based resources such as trimethylolpropane [3, 4], vanillin [5], isosorbide [6], sorbitol, glycerol [3], pentaerythritol [3], furfuryl glycidyl ether [7] and polytrimethylene ether glycols [8].

Currently, commercially available is also bio-based epichlorohydrin, which can pose a primary monomer for NIPU synthesis. Epichlorohydrin is an organic chemical compound from the group of epoxides containing a side chloromethyl group. Under industrial conditions, epichlorohydrin is obtained by chlorination of propylene to allyl chloride followed by epoxidation of the latter. 100% bio-based epichlorohydrin is produced using process based on glycerol (by-product from biodiesel production). It offers significant environmental advantages compared to epichlorohydrine from fossil fuel, in example 61% reduction in Global Warming Potential and 57% less energy consumption [9].

✉ Janusz Datta  
janusz.datta@pg.edu.pl

<sup>1</sup> Faculty of Chemistry, Department of Polymer Technology,  
Gdansk University of Technology, 11/12 Gabriela  
Narutowicza Street, 80-233 Gdansk, Poland

The impact of the use of monomers with different origin in the synthesis of NIPUs on their final properties and also on the course of synthesis is an interesting issue in the field of polymers. Moreover, the origin of monomers can also affect the thermal decomposition mechanism and its activation energy.

One of the most important information about the thermal stability of various polymers is their thermal degradation kinetics, which e.g. gives the information about the activation energy ( $E_a$ ) of material thermal decomposition. The thermal degradation kinetics can be determined based on thermogravimetric analysis. The majority of methods which allow for thermal decomposition kinetics determination are based on reaction models. These methods are difficult to use due to the sophisticated thermal degradation mechanisms of most polymers. Nevertheless, commonly known are also some methods which employ mathematical formulae without precise knowledge about decomposition reaction mechanisms, e.g. Kissinger [10, 11], Friedman [12, 13] or Ozawa, Flynn and Wall methods [14–16]. The last method from above-mentioned assumes that with the alteration of the heating rate  $\beta$ , the conversion function  $f(\alpha)$  stays constant for all values of conversion  $\alpha$ . This method consists of measurements of the temperatures attributable to the conversion  $\alpha$  from experiments carried out at different heating rates  $\beta$  (thermogravimetric analysis). The activation energy ( $E_a$ ) is determined according to the plot of  $\ln(\beta)$  versus  $1/T$  drawn up on the basis of Eq. (1) [17].

$$\ln(\beta) = \left[ \frac{AE_{app}}{Rg(\alpha)} \right] - 0.4567 \frac{E_{app}}{RT} - 2.315 \quad (1)$$

where:  $\beta$  – heating rate [ $\text{K min}^{-1}$ ];  $A$  – pre-exponential factor, that is assumed to be temperature independent;  $g(\alpha)$  – the integral reaction model;  $E_{app}$  – the approximate activation energy [ $\text{kJ mol}^{-1}$ ];  $T$  – temperature [ $\text{K}$ ];  $R$  – gas constant [ $8.314 \times 10^{-3} \text{ kJ mol}^{-1} \text{ K}^{-1}$ ].

Plotting  $\log \beta$  versus  $1/T$  creates linear trends at each fixed degree of conversion  $\alpha$ . The approximate activation energy is proportional to the slope of the plot's best-fit line, according to the relation (3):

$$\text{slope} = -0.4567 \frac{E_{app}}{R} \quad (2)$$

The main aim of this study was to determine the thermal degradation characteristics of the obtained semi-products and non-isocyanate polyurethanes on their basis. Thermal degradation characteristics was determined using thermogravimetric analysis (TGA). The kinetics of the thermal degradation was set according to Ozawa, Flynn, and Wall method (OFW). Non-isocyanate polyurethanes were synthesized via polyaddition reaction between bis (cyclic carbonate)s and dimerized fatty acids-based diamine derivatives.

The three-step synthesis pathway was carried out with the use of bio-based poly (trimethylene glycol) as a starting molecule. The present paper is also an attempt to bring more insight into the comparison and influence of the use of petrochemical-based and bio-based substrates on the selected properties, mainly chemical structure and thermal degradation characteristics of the synthesized semi-products and final NIPUs.

## Materials and methods

### Materials

For the syntheses, the following monomers and catalysts were used:

- bio-based poly(trimethylene glycol) (PO3G), Sensatis® (molecular mass:  $250 \text{ g mol}^{-1}$ ), purchased from Allesta (Germany),
- petrochemical-based epichlorohydrin (ECH; purity ca.  $\geq 99\%$ ; molecular mass:  $92.52 \text{ g mol}^{-1}$ ),
- bio-based epichlorohydrin (EPI; molecular mass:  $92.52 \text{ g mol}^{-1}$ ), purchased from Advanced Biochemical (Thailand),
- sodium hydroxide (NaOH) purchased from Sigma-Aldrich,
- boron trifluoride-diethyl ether complex ( $\text{BF}_3 \cdot \text{Et}_2\text{O}$ ) (purity ca.  $\geq 98\%$ ; molecular mass:  $141.93 \text{ g mol}^{-1}$ ), acquired from Sigma-Aldrich,
- tetrabutyl ammonium bromide (TBAB) (molecular mass:  $322.38 \text{ g mol}^{-1}$ ; revealed purity ca. 99%), acquired from TCI Chemicals (India),
- diamine derivatives of dimerized fatty acids (Pri-amine®1075), purchased from Croda (Netherlands).

All chemicals and solvents were used as received.

### General procedure for the synthesis of diglycidyl ethers (ED)

The syntheses of the diglycidyl ethers were performed according to the previous study [18]. The dried bio-based polyether polyol PO3G250 and  $\text{BF}_3 \cdot \text{Et}_2\text{O}$ , as a catalyst were first mixed and heated to  $80 \text{ }^\circ\text{C}$  in a 0.5 L glass reactor equipped with a mechanical stirrer, Liebig condenser and temperature controller. Next, ECH or EPI was continuously added, the molar ratio of PO3G to ECH or EPI equaled 1:3, and the reaction was stirred at stirring speed of 200 rpm and at the temperature of  $80 \text{ }^\circ\text{C}$ . The mixture was cooled down to  $50 \text{ }^\circ\text{C}$  after 8 h of reaction and 50% w/w aqueous solution of NaOH was added dropwise over ca. 5 h. Then, the solid precipitate was removed by filtration under reduced

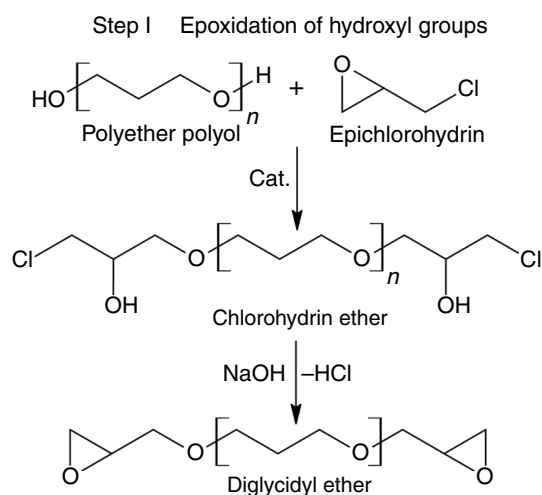


**Fig. 1** Scheme of the synthesis of diglycidyl ethers in the reaction between bio-based polyether polyol and epichlorohydrin

pressure. The product was extracted with ethyl acetate and then evaporated to remove solvents and unreacted compounds. The product ED250\_P was obtained as a colorless slightly viscous liquid with the use of petrochemical-based epichlorohydrin while ED250\_BIO was synthesized using bio-based epichlorohydrin. Figure 1 shows the scheme of the synthesis of diglycidyl ethers.

The  $^1\text{H}$  NMR spectra of two different types of epichlorohydrin (ECH and EPI) were compared and no additional protons were identified, which confirms the identical chemical structure of the used compounds.

$^1\text{H}$  NMR examination of the chemical structure of two types of epichlorohydrin was found: ECH (400 MHz,  $\text{DMSO-d}_6$ ),  $\delta$  (ppm) = 2.5 (DMSO- $\text{d}_6$  solvent signal), 2.7 (1H,  $-\text{CH}_2(\text{O})\text{CH}-\text{CH}_2-\text{Cl}$ ), 2.8 (1H,  $-\text{CH}_2(\text{O})\text{CH}-\text{CH}_2-\text{Cl}$ ), 3.2 (1H,  $-\text{CH}_2(\text{O})\text{CH}-\text{CH}_2-\text{Cl}$ ), 3.5 (1H,  $-\text{CH}_2-\text{Cl}$ ), 3.9 (1H,  $-\text{CH}_2-\text{Cl}$ );

EPI (400 MHz,  $\text{DMSO-d}_6$ ),  $\delta$  (ppm) = 2.5 (DMSO- $\text{d}_6$  solvent signal), 2.7 (1H,  $-\text{CH}_2(\text{O})\text{CH}-\text{CH}_2-\text{Cl}$ ), 2.8 (1H,  $-\text{CH}_2(\text{O})\text{CH}-\text{CH}_2-\text{Cl}$ ), 3.2 (1H,  $-\text{CH}_2(\text{O})\text{CH}-\text{CH}_2-\text{Cl}$ ), 3.5 (1H,  $-\text{CH}_2-\text{Cl}$ ), 3.9 (1H,  $-\text{CH}_2-\text{Cl}$ ).

### General procedure for the synthesis of bis(cyclic carbonate)s (DC)

Five-membered bis(cyclic carbonate)s were synthesized under the reaction of ED250\_P or ED250\_BIO with  $\text{CO}_2$ . The reaction was conducted in 0.5 L three-necked flask equipped with a temperature controller, a magnetic stirrer, and an inlet of  $\text{CO}_2$  [18]. The TBAB (0.5 mass%) as a catalyst was added to the reaction mixture and the temperature was heated to 110  $^\circ\text{C}$ . The reaction was conducted for 30 h under atmospheric pressure with a 100 mL  $\text{min}^{-1}$   $\text{CO}_2$  gas flow rate. The obtained product was analyzed in detail and

used for NIPU preparation without further purification. The produced DC250\_P and DC250\_BIO were colorless liquids at room temperature. Figure 2 shows the scheme of the synthesis of bis(cyclic carbonate)s.

### General procedure for the synthesis of non-isocyanate polyurethanes (NIPUs)

One-pot polyaddition reaction between DC and dimerized fatty acids-based diamine derivatives (Priamine 1071, amine value of 193 mg  $\text{KOH g}^{-1}$ , [18], dimer/trimer content of 3/1 and average amine functionality of 2.2 [19]) were used for NIPUs preparation. The mixture of DC250\_P or DC250\_BIO and Priamine 1071 in molar ratio 1:1.2, was mechanically stirred for 3 h at 110  $^\circ\text{C}$ . Then, the reactive mixture was placed into a mold and cured at 110  $^\circ\text{C}$  for 48 h in a laboratory oven. The prepared NIPU was denoted as NIPU250\_P and NIPU250\_BIO. Figure 3 shows the scheme of the synthesis of non-isocyanate polyurethanes.

### Measurements

#### Fourier transform infrared spectroscopy (FTIR)

The chemical structure of the obtained semi-products and NIPUs was verified by means of a Nicolet 8700 FTIR Spectrophotometer (Thermo Electron Corporation, USA) with the attenuated total reflection sampling technique ATR. All samples were measured at room temperature in the wavenumber range from 4500 to 500  $\text{cm}^{-1}$ . The spectra were collected using 64 scans with a resolution of 4  $\text{cm}^{-1}$ .

#### Nuclear magnetic resonance ( $^1\text{H}$ NMR)

$^1\text{H}$  NMR spectra allowed for semi-products and NIPUs chemical structure confirmation and were recorded on

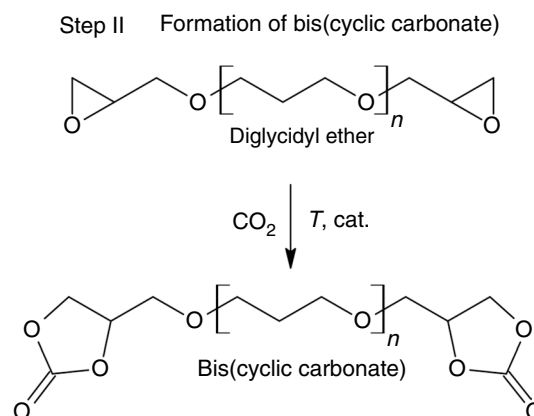
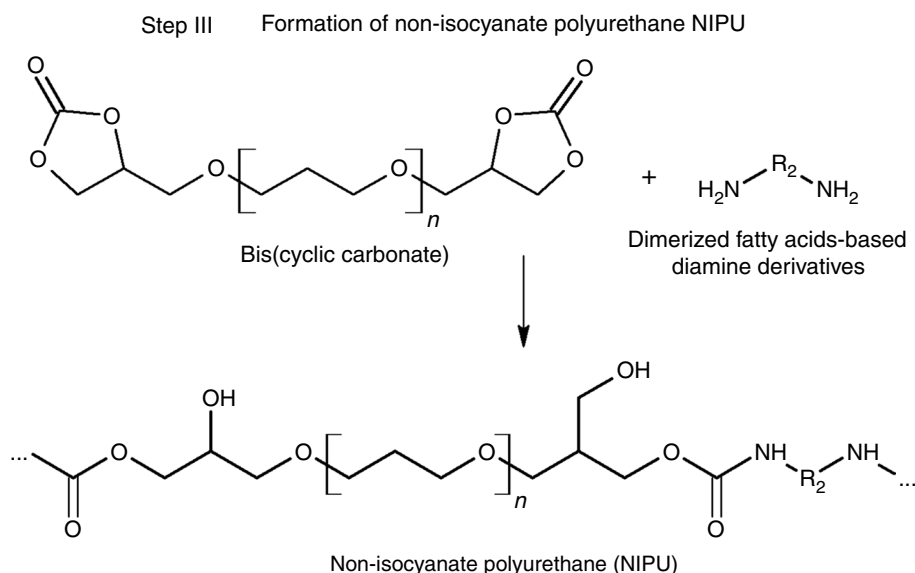


**Fig. 2** Scheme of the synthesis of bis(cyclic carbonate)s in the cycloaddition of  $\text{CO}_2$  into diglycidyl ether

**Fig. 3** Scheme of the synthesis of non-isocyanate polyurethanes in the reaction between bis(cyclic carbonate) and dimerized fatty acids-based diamine derivatives



Varian Mercury Vx spectrometer. All samples were measured at ambient temperature with a frequency of 400 MHz. DMSO- $d_6$  was used as a solvent and TMS as an external standard.

#### Size exclusion chromatography (SEC)

To determine the number ( $M_n$ ) and mass ( $M_w$ ) average molecular masses, as well as the dispersity of the obtained semi-products and NIPUs, the size exclusion chromatography was performed. A chromatographic system equipped with a refractive index detector (Shodex, Japan), UV-Vis detector (1  $\frac{1}{4}$  254 nm, LCD 2084; Ecom, Czech Republic) and a set of three columns (PL gel with a particle size of 10 mm, pore size: 50/ 10E3/10E4 Å, 7.5 mm, Polymer laboratories, UK) was used. The samples were analyzed as a solution in THF at 30 °C and a flow rate of 1 mL  $\text{min}^{-1}$ . Samples were filtered before testing using 2  $\mu\text{m}$  pore size nylon filters. The elution times were converted to molecular mass using a calibration with polystyrene (PS) standard.

#### Thermogravimetric analysis (TGA)

Thermogravimetric Analysis was realized using NETZSCH TG 209 F3 Thermogravimetric Analyzer. The samples (ca. 10 mg) were placed in a corundum crucible and heated from room temperature to 700 °C at various heating rates: 5, 10, and 20 °C  $\text{min}^{-1}$ . The measurements were realized under continuous nitrogen flow ( $\text{N}_2$ ). Under these conditions, the experiments were sufficiently reproducible.

## Results and discussion

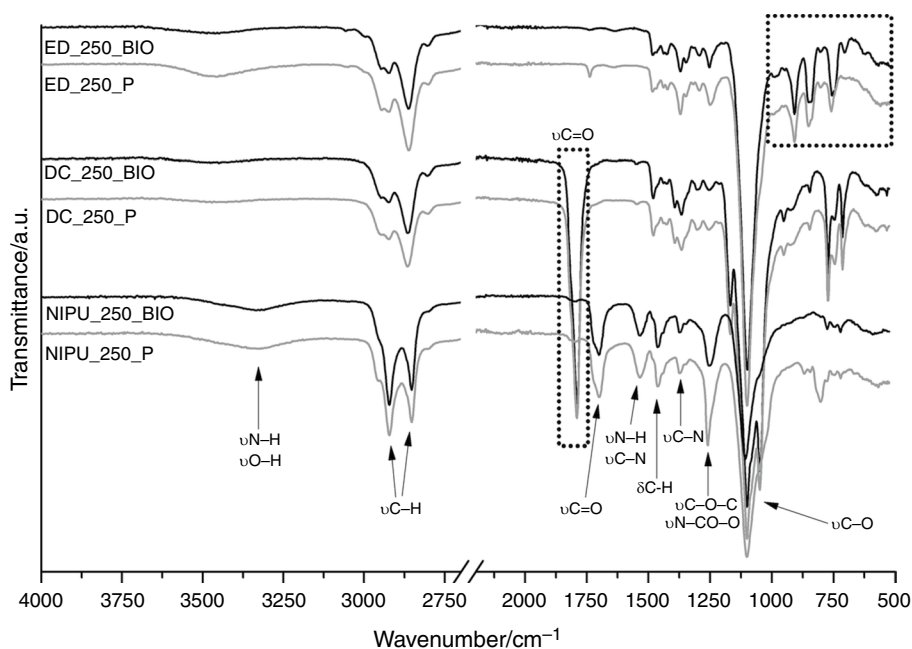
### Chemical structure characterization (FTIR, $^1\text{H}$ NMR)

The chemical structures of the synthesized compounds were analyzed by FTIR and  $^1\text{H}$  NMR methods. The FTIR spectra (Fig. 4) have confirmed the successful epoxidation reaction which is due to the appearance of two bands at 908  $\text{cm}^{-1}$  ( $\nu\text{C}-\text{O}$  of the oxirane group) and 841  $\text{cm}^{-1}$  ( $\nu\text{C}-\text{O}-\text{C}$  of the oxirane group). The disappearance of the absorption band characteristic for the vibrations of the hydroxyl groups present in the polyol structure is also visible (3590–3310  $\text{cm}^{-1}$ ). Spectra of diglycidyl ethers (ED) also contained typical bands of asymmetric and symmetric stretching vibrations of C-H groups ( $\nu-\text{CH}_2-$  and  $\nu-\text{CH}_3$ ) at 2930 and 2850  $\text{cm}^{-1}$  and ether group stretching vibrations ( $\nu-\text{C}-\text{O}-\text{C}-$ ) at 1100  $\text{cm}^{-1}$ . The epoxy band characteristic for the diglycidyl ethers chemical structure (epoxy region) was recognized on both spectra, regardless of the used epichlorohydrin (bio-based or petrochemical-based one). According to  $^1\text{H}$  NMR examination of the chemical structure of diglycidyl ether was found:

ED\_250\_BIO (400 MHz, DMSO- $d_6$ ),  $\delta$  (ppm) = 1.7 (m, 10H,  $-\text{CH}_2-$  polyol chain), 2.55 (m, 2H,  $-\text{CH}_2(\text{O})\text{CH}-$  epoxy group, estimated values, overlapped with solvent signal), 2.72 (m, 2H,  $-\text{CH}_2(\text{O})\text{CH}-$  epoxy group), 3.08 (m, 1.89H,  $-\text{CH}_2(\text{O})\text{CH}-$  epoxy group), 3.2 (m, 1.4H,  $-\text{CH}_2(\text{O})\text{CH}-\text{CH}_2-\text{O}-$ ), 3.95–3.26 (m, 89.5H,  $-\text{CH}_2(\text{O})\text{CH}-\text{CH}_2-\text{O}-$ ,  $-\text{O}-\text{CH}_2-\text{CH}_2-\text{CH}_2-\text{O}-$  polyol chain, overlapped with  $\text{H}_2\text{O}$  and side products);

ED\_250\_P (400 MHz, DMSO- $d_6$ ),  $\delta$  (ppm) = 1.7 (m, 10H,  $-\text{CH}_2-$  polyol chain), 2.56 (m, 2H,  $-\text{CH}_2(\text{O})\text{CH}-$  epoxy group, estimated values, overlapped with solvent signal), 2.72 (m, 2H,  $-\text{CH}_2(\text{O})\text{CH}-$  epoxy group), 3.09 (m, 2H,  $-\text{CH}_2(\text{O})$ )

**Fig. 4** The FTIR spectra of diglycidyl ethers, bis(cyclic carbonate)s and non-isocyanate polyurethanes synthesized using two types of epichlorohydrin—ECH and EPI



CH<sub>2</sub>-epoxy group), 3.6 (m, 1.5H, -CH<sub>2</sub>(O)CH-CH<sub>2</sub>-O-), 3.95–3.26 (m, 111.52H, -CH<sub>2</sub>(O)CH-CH<sub>2</sub>-O-, -O-CH<sub>2</sub>-CH<sub>2</sub>-CH<sub>2</sub>-O<sub>polyol chain</sub>, overlapped with H<sub>2</sub>O and side products), 5.27 (d, 0.5H, -OH<sub>side product</sub>).

All resonance signals have been assigned to the corresponding protons based on the integration values. In our previous studies, we proved that besides the main product, additional by-products were identified to have formed during the epoxidation, as evidenced by the signal at the chemical shift  $\delta = 5.27$  in the case of ED\_250\_P [8]. This signal is not identified for ED\_250\_BIO sample.

The cycloaddition of CO<sub>2</sub> into diglycidyl ethers, which led to bis(cyclic carbonate)s, was performed under optimized conditions determined in our previous studies [8, 18, 20]. The FTIR spectra of the DC\_250\_BIO and DC\_250\_P samples demonstrate disappearance of the band at 915 cm<sup>-1</sup> which proves that CO<sub>2</sub> is incorporated into the epoxy groups in the chemical structure of diglycidyl ethers. The complete disappearance of this band cannot be confirmed due to the overlap of the band characteristic of in-plane bending vibration of methyl group [21]. Spectra also contained a typical distinctive absorption peak at 1800 cm<sup>-1</sup> corresponding to the stretching vibration of carbonyl groups ( $\nu$ C=O) which confirms the formation of the assumed structure of cyclic carbonates (cyclic carbonate groups). According to <sup>1</sup>H NMR examination of the chemical structure of bis(cyclic carbonate)s was found: DC\_250\_BIO (400 MHz, DMSO-d<sub>6</sub>),  $\delta$  (ppm) = 1.7 (m, 10.36H, -CH<sub>2</sub>-<sub>polyol chain</sub>), 2.5 (DMSO-d<sub>6</sub> solvent signal), 3.27–3.94 (m, 99.93H, cyclic carbonate-CH<sub>2</sub>-O-, -O-CH<sub>2</sub>-CH<sub>2</sub>-CH<sub>2</sub>-O<sub>polyol chain</sub>, overlapped with H<sub>2</sub>O and side products), 4.26 (m, 2H, -CH<sub>2</sub>O<sub>cyclic carbonate</sub>),

4.53 (m, 2H, -CH<sub>2</sub>O<sub>cyclic carbonate</sub>), 4.91 (m, 2H, -CHO<sub>cyclic carbonate</sub>), 5.25 (d, 0.27H, -OH<sub>side product</sub>); DC\_250\_P (400 MHz, DMSO-d<sub>6</sub>),  $\delta$  (ppm) = 1.71 (m, 11.26H, -CH<sub>2</sub>-<sub>polyol chain</sub>), 2.5 (DMSO-d<sub>6</sub> solvent signal), 3.27–3.94 (m, 119.52H, cyclic carbonate-CH<sub>2</sub>-O-, -O-CH<sub>2</sub>-CH<sub>2</sub>-CH<sub>2</sub>-O<sub>polyol chain</sub>, overlapped with H<sub>2</sub>O and side products), 4.26 (m, 2H, -CH<sub>2</sub>O<sub>cyclic carbonate</sub>), 4.52 (m, 2H, -CH<sub>2</sub>O<sub>cyclic carbonate</sub>), 4.91 (m, 2H, -CHO<sub>cyclic carbonate</sub>), 5.26 (d, 1.43H, -OH<sub>side product</sub>).

FTIR analysis was also used to confirm the final structure of non-isocyanate polyurethanes. The characteristic absorption bands of functional groups were identified. Both synthesized materials showed the characteristic groups for polyurethanes, suggesting a quite similar chemical structure. Almost complete disappearance of the typical carbonyl group stretching vibration absorption band at 1790 cm<sup>-1</sup> was observed. It indicates that during the reaction bis(cyclic carbonate)s quantitatively convert into polyurethane materials [22]. The appearance of new urethane linkage bands, i.e. C=O (1695 cm<sup>-1</sup>), N-H (1535 cm<sup>-1</sup>) and C-N (1367 cm<sup>-1</sup>), and the C-O asymmetric stretching vibration band of N-CO-O and C-O-C linkages at about 1258 cm<sup>-1</sup> also verified the complete conversion of cyclic carbonate groups [1, 3]. The broad absorption bands at 3333 cm<sup>-1</sup> are related to the O-H and N-H stretching vibrations [23]. New peak appearing at around 1098 cm<sup>-1</sup> corresponds to the C-O-C (polyether polyol chain) vibration of the polyol chain. According to FTIR spectra, the final conversion of the cyclic carbonate groups was estimated to 92% and 89% for NIPU\_250\_BIO and NIPU\_250\_P, respectively. The conversion was estimated by the relative absorption intensity of the carbonyl ( $\nu$ C=O) to methyl groups ( $\nu$ C-H) vibrations in



the chemical structure of bis(cyclic carbonate)s and NIPU materials [24].

### Molecular mass characterization

The number and mass average molecular masses and dispersity of the semi-products for NIPUs obtainment were determined with the use of size exclusion chromatography. The number average molecular mass is defined as the total mass of the polymer divided by the total number of molecules. Therefore, the theoretical  $M_n$  of the synthesized bis(cyclic carbonate)s was calculated from the  $M_n$  values of the initial bio-based poly(trimethylene glycol), PO3G250. The calculation was performed based on the assumption of full conversion and occurrence of no side reactions. Table 1 presents the values of theoretical number average molecular mass, number and mass average molecular masses and dispersity.

**Table 1** Theoretical number ( $M_n$ ) average molecular mass, number ( $M_n$ ) and mass ( $M_w$ ) average molecular mass and dispersity ( $\mathcal{D}$ ) from SEC measurements of the synthesized diglycidyl ethers ED250 and bis(cyclic carbonate)s DC250

Sample	$M_n$ /Da (theoretical)	$M_n$ /Da /SEC	$M_w$ /Da /SEC	$\mathcal{D}$ [- /SEC
ED_250_BIO	362	575	770	1.3
ED_250_P		524	740	1.4
DC_250_BIO	450	755	917	1.2
DC_250_P		747	905	1.2

Experimentally determined  $M_n$  values are in good agreement with the theoretical  $M_n$ . The difference in molecular mass verifies the occurrence of side reactions as confirmed by FTIR and NMR analyses. The differences between the theoretical and determined  $M_n$  molecular mass were higher in the case of bio-based semi-products than ED650, which agrees well with the above-mentioned findings that the side reactions proceed to a higher extent during DC250 synthesis. Nevertheless, in the second NIPUs synthesis step, obtained bis(cyclic carbonate)s characterized lower values of dispersity, which may indicate that the reaction of the second stage of the synthesis occurs in the direction of products with similar average molar mass.

### Thermogravimetric analysis (TGA)

Thermogravimetric analyses were performed to evaluate the thermal properties of the synthesized materials. The results confirmed their high thermal stability. Figure 5 presents the thermogravimetric curve (the TGA curve) and the first derivative of the TGA curve (the DTG curves) for relevant materials. The results confirmed one-step mechanism of the thermal degradation of semi-products and two-step degradation mechanism for the obtained NIPUs. The use of monomers with different origins – bio-based and petrochemical-based, visibly affects the course of the thermogravimetric curves, which make differences in the thermal stability characteristics (Table 2). All measured materials were thermally stable up to ca. 200 °C with the initial decomposition temperature ( $T_{5\%}$ ) of 203 and 220 °C for ED\_250\_P and ED\_250\_BIO, respectively, 241 and 246 °C for DC\_250\_BIO and DC\_250\_P, respectively, and 263 and 274 °C for

**Fig. 5** TG and DTG curves of the semi-products and obtained NIPUs

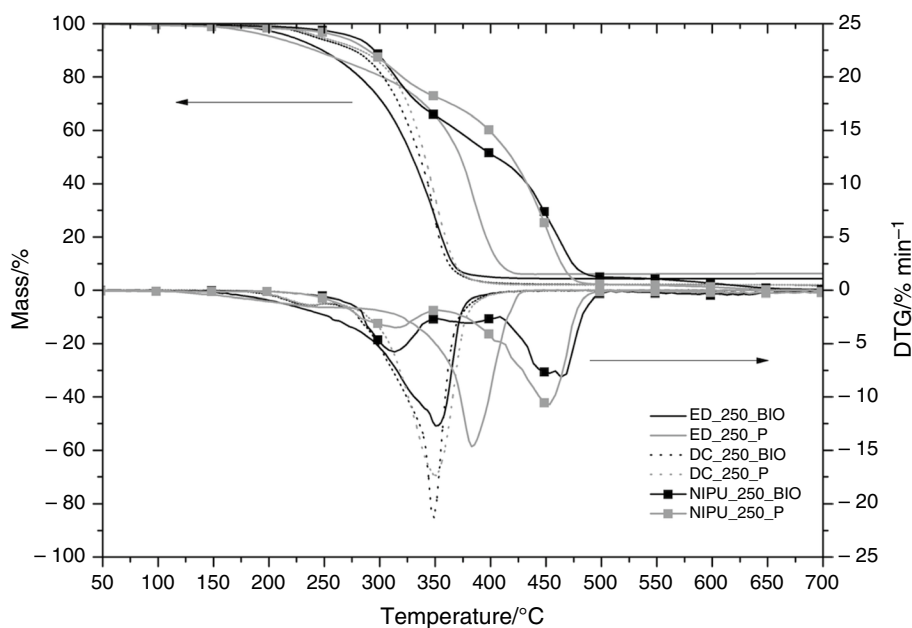


**Table 2** Summary of the thermal degradation behaviors of the obtained diglycidyl ethers, ED\_250, bis(cyclic carbonate)s, DC\_250 and the prepared non-isocyanate polyurethanes, NIPU\_250

Sample	T <sub>5%</sub> /°C	T <sub>50%</sub> /°C	T <sub>90%</sub> /°C	T <sub>max1</sub> /°C	T <sub>max2</sub> /°C	Solid residue at 650 °C /%
ED_250_BIO	220	330	365	350	–	4.4
ED_250_P	203	373	408	383	–	6.1
DC_250_BIO	241	336	361	346	–	2.0
DC_250_P	246	3414	369	351	–	2.0
NIPU_250_BIO	274	294	474	313	463	0.8
NIPU_250_P	263	288	419	313	453	0.1

NIPU\_250\_P and NIPU\_250\_BIO, respectively. The thermal degradation of NIPU\_250 was shown to proceed in two main steps, typical for these types of polyurethane materials [17, 25]. The first mass loss occurs at ca. 313 °C for both obtained NIPUs and corresponds to the degradation of the urethane linkages, while the second mass loss is attributed to the decomposition of soft segments – poly(trimethylene oxide) chains and occurs at 453 and 463 °C (T<sub>max2</sub>) for NIPU\_250\_P and NIPU\_250\_BIO, respectively [8].

Moreover, there are visible differences related to the intensity of the DTG curves, what gives information about the rate of mass loss of materials. For products of the first step of the NIPU synthesis, the petrochemical-based diglycidyl ether ED\_250\_P degrades faster than their bio-based counterparts. For bis(cyclic carbonate)s, it was bio-based DC\_250 in which the rate of mass loss was higher. In the case of NIPUs, which are characterized by two-step decomposition, at the first decomposition step at ca. 313 °C NIPU\_250\_BIO revealed a higher rate of mass loss related to the degradation of the urethane linkage. In the second degradation step, at 463 and 453 °C, for NIPU\_250\_BIO and NIPU\_250\_P, respectively, soft segments from petrochemical-based NIPU revealed a higher speed of mass loss.

### Thermal degradation kinetics

Thermal degradation kinetics of the products from each step of the three-step synthesis of NIPUs were determined with the use of model-free Ozawa, Flynn and Wall method. Figure 6 shows the Ozawa, Flynn and Wall plots prepared for diglycidyl ethers—ED\_250\_P and ED\_250\_BIO, bis(cyclic carbonate)s—DC\_250\_P and DC\_250\_BIO and obtained NIPUs—NIPU\_250\_P and NIPU\_250\_BIO. The straight lines are given which slope is proportional to the activation energy (-Ea/R). When the activation energy Ea increases with the increase of the conversion degree, the complex reaction mechanism can be confirmed. The single-step reaction can be verified if the determined activation energy Ea is the same for the different  $\alpha$  conversion values [14, 26].

Table 3 presents the activation energy, Ea, for all described materials with various degradation conversion,  $\alpha$ . The presented findings demonstrate that the activation

energy determined by OFW method shows a distinct dependence on the NIPU synthesis step. An increase in activation energy values for the degradation conversion  $\alpha$  equaling 0.05, was observed with each subsequent step in the synthesis of NIPUs. This means that at each subsequent stage of the synthesis, materials with higher activation energy of the thermal degradation reaction were obtained. The changes in this trend are visible at  $\alpha$  equaling 0.95. For this value of conversion, NIPUs revealed lower activation energy, Ea, then products from the second step of synthesis—bis(cyclic carbonate)s.

Moreover, based on the results shown in Table 3, it is visible that semi-products obtained with the use of bio-based monomers revealed higher values of activation energy, Ea of thermal decomposition in the initial range of degradation conversion,  $\alpha$ , (from 0.05 to 0.2) than their petrochemical countertype. Bis(cyclic carbonate)s based on bio-based monomers characterized higher values of Ea in full range of  $\alpha$ . The change at the Ea values for diglycidyl ethers occurs when higher values of the degradation conversion,  $\alpha$  are reached, higher than 0.5. The change at the Ea values for NIPUs occurs when the degradation conversion,  $\alpha$  reached higher values than 0.3. Then the petrochemical products show higher Ea values with successive  $\alpha$ . At the initial stage of distribution for NIPUs, Ea remains high values which are associated with the dissociation of urethane bonds [27–29]. The highest value of Ea in this area was recorded for NIPU\_250\_BIO material which may suggest a higher content of urethane bonds in the polyurethane chemical structure. For bond dissociation reactions in the range of 0.3–0.5 conversion corresponds to a single dominant kinetic process associated with decomposition of soft segments. After exceeding 0.5 of degradation conversion, there was registered a significant increase in Ea for NIPU\_250\_P related to a dissociation energy of chemical bonds of the compounds produced by the secondary reactions during the decomposition of the structure of PUR. Nevertheless, after exceeding 0.5 of degradation conversion, for NIPU\_250\_BIO there was registered a decrease in Ea. The results may suggest that secondary reactions do not occur in this case or the activation energy of these reactions has been achieved in the range of lower values of degradation conversion,  $\alpha$ .

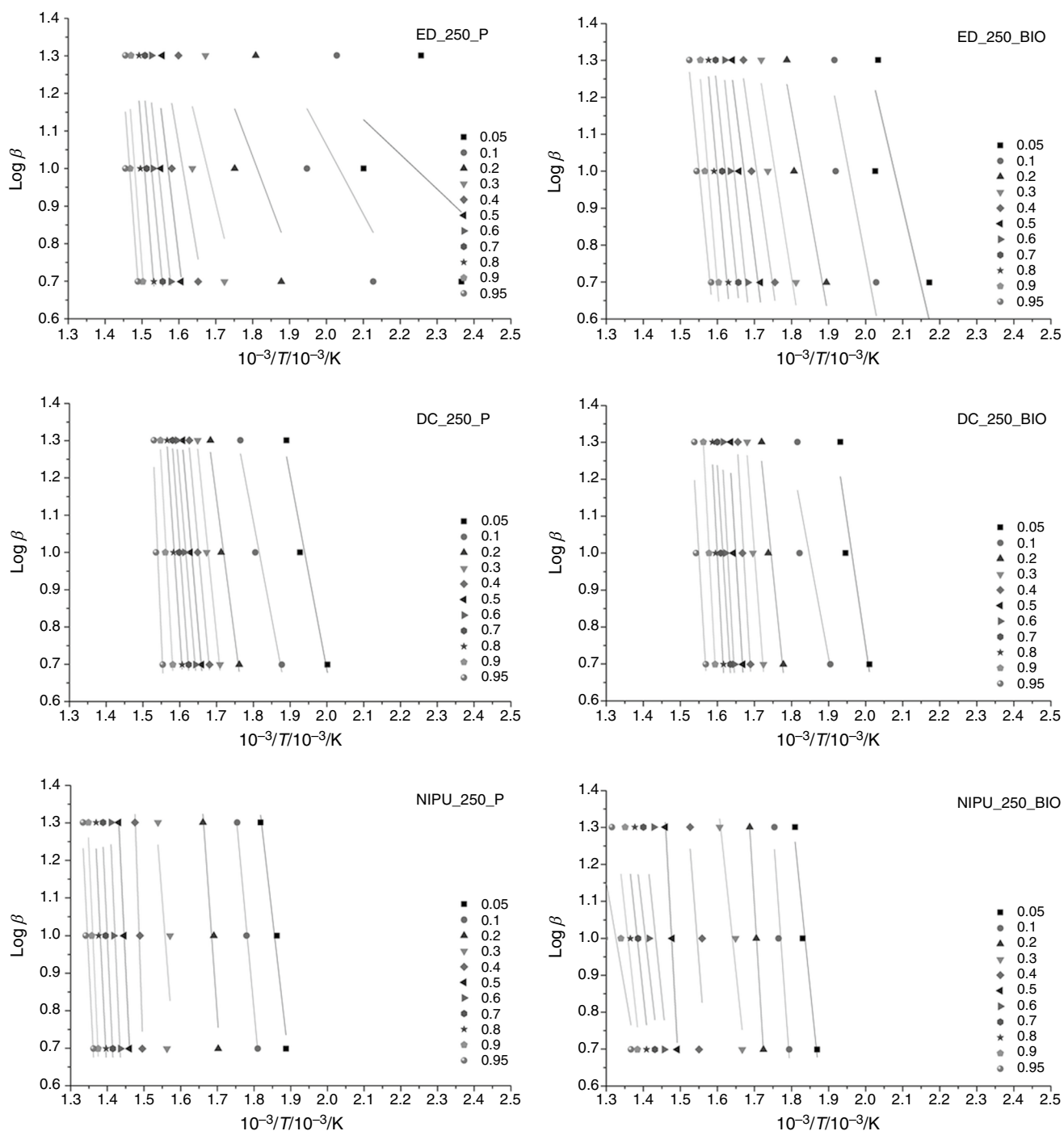


**Fig. 6** Ozawa, Flynn and Wall plots of the semi-products and prepared NIPUs

Typically,  $E_a$  maximized at end of conversion (in the range of  $\alpha$  between 0.7 to 0.9) which is related with C–C bond dissociation. This phenomenon is visible for diglycidyl ethers and bis(cyclic carbonate)s. Interesting is the fact that for NIPUs, in the range of  $\alpha$  between 0.7 and 0.9 the  $E_a$  values decrease. For bio-based NIPU,  $E_a$  at the value of  $\alpha$  at 0.9, equaled 168.7 kJ mol<sup>-1</sup>, when for petrochemical-based

NIPU,  $E_a$  equaled 397.3 kJ mol<sup>-1</sup> at the same conversion. The higher value of  $E_a$  for NIPU\_250\_P during heating might be related to higher heat absorption process, resulting due to the presence of higher NCO groups. Probably, in this material, the mobility of macromolecules was reduced, and higher energy level was needed for their vibration [30].





**Table 3** Energy of thermal degradation activation of the products of three steps of NIPU production

Degradation conversion, $\alpha$	Thermal degradation activation energy, $E_a$ , /kJ mol <sup>-1</sup>					
	ED_250_BIO	ED_250_P	DC_250_BIO	DC_250_P	NIPU_250_BIO	NIPU_250_P
0.05	56.2	16.9	122.7	94.9	177.2	153.9
0.1	74.9	33.4	98.3	95.0	257.5	194.5
0.2	90.2	47.5	177.8	137.0	296.4	249.2
0.3	103.7	73.7	242.2	177.8	171.1	230.2
0.4	119.4	105.7	313.6	197.6	233.8	530.2
0.5	132.4	149.2	299.7	210.6	339.6	374.5
0.6	160.9	169.1	327.1	217.3	175.0	407.9
0.7	168.0	187.9	289.9	248.1	157.9	384.4
0.8	192.4	223.4	348.0	267.4	171.0	372.4
0.9	204.6	241.3	346.5	322.3	168.7	397.3
0.95	180.9	242.7	306.7	415.2	105.3	357.3

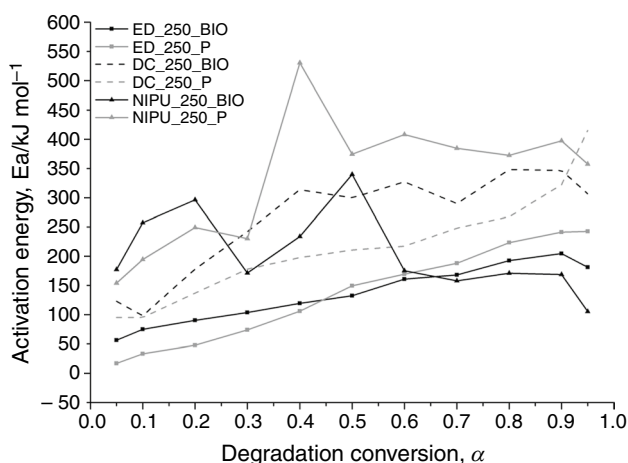
**Fig. 7** Dependence of the activation energy ( $E_a$ ) on the relative extent of degradation ( $\alpha$ ), as calculated with OFW method for products obtained from three steps of the NIPUs synthesis

Figure 7 shows the dependence of the activation energy ( $E_a$ ) on the relative extent of degradation conversion, as calculated with OFW methods for all described materials. The comparison confirmed the similarity at the curve courses for plots characterizing the same material groups – similar curve courses for diglycidyl ethers, bis(cyclic carbonate)s and NIPUs. Noteworthy is the fact that the profiles of the wave forms of the characteristic curves for the same group of compounds, i.e. diglycidyl ethers, bis(cyclic carbonate)s and NIPUs are similar.

The comparison of the activation energy of the obtained NIPUs with the polyurethane materials obtained via isocyanate route revealed differences in the values of  $E_a$  at the beginning of thermal decomposition ( $\alpha$  in the range between 0.1 and 0.3) which are usually in the range from 100 to 200 kJ mol<sup>-1</sup> for typical polyurethanes [31, 32]. The obtained NIPUs characterized higher activation energy,  $E_a$  at the beginning of thermal decomposition which can

be related to that the higher energy must be achieved for the dissociation of urethane bonds. The  $E_a$  values for the polyurethane materials obtained via isocyanate route at the end of thermal decomposition ( $\alpha$  in the range between 0.7 and 0.9) ranged between 150 and 350 kJ mol<sup>-1</sup> [33]. This range is similar to bio-based non-isocyanate polyurethanes but lower than  $E_a$ -characterized petrochemical-based NIPU. The results prove that more energy is needed to degrade NIPU\_250\_P material to a greater degree of conversion.

Based on the thermal decomposition kinetics study results, it can be concluded that bio-based NIPUs are competitive with their petrochemical counterparts due to higher activation energy at the beginning of thermal decomposition and lower  $E_a$  at the end of the thermal degradation than petrochemical-based NIPU.

## Conclusions

In this work, bio-based monomers such as bio-polyether polyol, bio-epichlorohydrin, and bio-based amine hardener were utilized in order to develop a green route to fully bio-based non-isocyanate polyurethanes. Two types of epichlorohydrin were compared in this research work—ECH and EPI. The first one is obtained on an industrial scale by the traditional method of using petrochemical-based resources (ECH), while the second one is synthesized using waste glycerin from biodiesel production (EPI). The chemical structure of the obtained intermediates and the final materials was compared with the use of spectroscopic methods. It was found that in both cases epoxidation reactions revealing the formation of epoxy groups (ED\_250\_P and ED\_250\_BIO samples) were successfully performed. Moreover, the chemical fixation of CO<sub>2</sub> into the chemical structure of diglycidyl ethers was carried out with great success. It is worth noting that the proposed method of bis(cyclic carbonate)s synthesis does not require the use of increased

pressure and toxic organic solvents. The high potential of the obtained cyclic carbonates in the synthesis of polyurethanes has also been demonstrated. FTIR analysis was confirmed the final intended structure of crosslinked NIPUs.

The results of size exclusion chromatography verified similarity in the number and mass average molecular mass of the synthesized semi-products for NIPUs obtainment. Bio-based or petrochemical-based epichlorohydrin did not affect significantly the semi-products molecular masses and their dispersity. Diglycidyl ethers—ED\_250\_P and ED\_250\_BIO, revealed the number average molecular mass at ca. 550 Da, when bis(cyclic carbonate)s—DC\_250\_P and DC\_250\_BIO, characterized number average molecular mass at ca. 750 Da. Higher values of  $M_n$  for these products are related probably to side reactions that can occur during diglycidyl ethers and bis(cyclic carbonate)s synthesis.

Thermogravimetric analyses confirmed the thermal stability of the semi-products above 200 °C. Moreover, NIPUs materials revealed two-step decomposition which is characteristic of polyurethane materials. Based on the thermal decomposition kinetics results it can be concluded that bio-based NIPUs are competitive with their petrochemical counterparts due to higher activation energy,  $E_a$  at the beginning of thermal decomposition than petrochemical epichlorohydrin-based NIPUs.

**Acknowledgements** The authors wish to thank Allesta (Germany) for kindly providing bio-based polyether polyols (Sensatis® and Velvetol®) samples used in this study. The authors are also grateful to Croda International (Netherlands) for supplying the diamine derivative of dimerized fatty acids (Priamine®) samples. We would like to express our sincere thanks to Advanced Biochemical (Thailand) for providing Bio-based Epichlorohydrin.

## Declarations

**Conflict of interest** The authors declare that they have no conflict of interest.

**Open Access** This article is licensed under a Creative Commons Attribution 4.0 International License, which permits use, sharing, adaptation, distribution and reproduction in any medium or format, as long as you give appropriate credit to the original author(s) and the source, provide a link to the Creative Commons licence, and indicate if changes were made. The images or other third party material in this article are included in the article's Creative Commons licence, unless indicated otherwise in a credit line to the material. If material is not included in the article's Creative Commons licence and your intended use is not permitted by statutory regulation or exceeds the permitted use, you will need to obtain permission directly from the copyright holder. To view a copy of this licence, visit <http://creativecommons.org/licenses/by/4.0/>.

## References

- Lamarzelle O, Hibert G, Lecommandoux S, Grau E, Cramail H. A thioglycerol route to bio-based bis-cyclic carbonates: Poly(hydroxyurethane) preparation and post-functionalization. *Polym Chem.* 2017;8:3438–47.
- Błażek K, Datta J. Renewable natural resources as green alternative substrates to obtain bio-based non-isocyanate polyurethanes—review. *Crit Rev Environ Sci Technol.* 2019;49:173–211.
- Fleischer M, Blattmann H, Mühlaupt R. Glycerol-, pentaerythritol- and trimethylolpropane-based polyurethanes and their cellulose carbonate composites prepared via the non-isocyanate route with catalytic carbon dioxide fixation. *Green Chem.* 2013;15:934–42.
- Camara F, Benyahya S, Besse V, Boutevin G, Auvergne R, Boutevin B, et al. Reactivity of secondary amines for the synthesis of non-isocyanate polyurethanes. *Eur Polym J.* 2014;55:17–26. <https://doi.org/10.1016/j.eurpolymj.2014.03.011>.
- Fache M, Darroman E, Besse V, Auvergne R, Caillol S, Boutevin B. Vanillin, a promising biobased building-block for monomer synthesis. *Green Chem.* 2014;16:1987–98.
- Besse V, Auvergne R, Carlotti S, Boutevin G, Otazaghine B, Caillol S, et al. Synthesis of isosorbide based polyurethanes: An isocyanate free method. *React Funct Polym.* 2013;73:588–94. <https://doi.org/10.1016/j.reactfunctpolym.2013.01.002>.
- Karami Z, Zohuriaan-Mehr MJ, Rostami A. Bio-based thermo-healable non-isocyanate polyurethane DA network in comparison with its epoxy counterpart. *J CO<sub>2</sub> Util.* 2017;18:294–302. <https://doi.org/10.1016/j.jcou.2017.02.009>.
- Błażek K, Beneš H, Walterová Z, Abbrent S, Eceiza A, Calvo-Correas T, et al. Synthesis and structural characterization of bio-based bis(cyclic carbonate)s for the preparation of non-isocyanate polyurethanes. *Polym Chem.* 2021;12:1643–52.
- Ricciardi M, Cespi D, Celentano M, Genga A, Malitesta C, Proto A, et al. Bio-propylene glycol as value-added product from Epicerol® process. *Sust Chem Pharm.* 2017;6:10–3.
- Starink MJ. The determination of activation energy from linear heating rate experiments: a comparison of the accuracy of isoconversion methods. *Thermochim Acta.* 2003;404:163–76.
- Semsarzadeh MA, Navarchian AH. Effects of NCO/OH ratio and catalyst concentration on structure, thermal stability, and cross-link density of Poly (urethane-isocyanurate). *J Appl Polym Sci.* 2003;90:963–72.
- Chrissafis K, Paraskevopoulos KM, Bikiaris DN. Thermal degradation mechanism of poly (ethylene succinate) and poly (butylene succinate): comparative study. *Thermochim Acta.* 2005;435:142–50.
- Yao F, Wu Q, Lei Y, Guo W, Xu Y. Thermal decomposition kinetics of natural fibers: activation energy with dynamic thermogravimetric analysis. *Polym Degrad Stab.* 2008;93:90–8.
- Chrissafis K, Paraskevopoulos KM, Bikiaris DN. Thermal degradation kinetics of the biodegradable aliphatic polyester, poly(propylene succinate). *Polym Degrad Stab.* 2006;91:60–8.
- Venkatesh M, Ravi P, Tewari SP. isoconversional kinetic analysis of decomposition of Nitroimidazoles: Friedman method vs Flynn – Wall – Ozawa Method. *J Phys Chem A.* 2013;117:10162–9.
- Parcheta P, Koltsov I, Datta J. Fully bio-based poly(propylene succinate) synthesis and investigation of thermal degradation kinetics with released gases analysis. *Polym Degrad Stab.* 2018;151:90–9.
- Rowe AA, Tajvidi M, Gardner DJ. Thermal stability of cellulose nanomaterials and their composites with polyvinyl alcohol (PVA). *J Therm Anal Calorim.* 2016;126:1371–86.
- Błażek K, Kasprzyk P, Datta J. Diamine derivatives of dimerized fatty acids and bio-based polyether polyol as sustainable platforms for the synthesis of non-isocyanate polyurethanes. *Polymer (Guildf).* 2020;205:1–14.
- Carré C, Bonnet L, Avérous L. Solvent- and catalyst-free synthesis of fully biobased nonisocyanate polyurethanes with different macromolecular architectures. *RSC Adv.* 2015;5:100390–400.

20. Błażek K, Datta J, Cichoracka A. Sustainable synthesis of cyclic carbonates from bio-based polyether polyol: the structure characterization, rheological behaviour and thermal properties. *Polym Int.* 2019;68(12):1968–79.
21. Ke J, Li X, Wang F, Kang M, Feng Y, Zhao Y, et al. The hybrid polyhydroxyurethane materials synthesized by a prepolymerization method from CO<sub>2</sub>-sourced monomer and epoxy. *J CO<sub>2</sub> Util.* 2016;16:474–85.
22. Carré C, Zoccheddu H, Delalande S, Pichon P, Avérous L. Synthesis and characterization of advanced biobased thermoplastic nonisocyanate polyurethanes, with controlled aromatic-aliphatic architectures. *Eur Polym J.* 2016;84:759–69.
23. Janvier M, Ducrot PH, Allais F. Isocyanate-free synthesis and characterization of renewable Poly(hydroxy)urethanes from Syringaresinol. *ACS Sust Chem Eng.* 2017;5:8648–56.
24. Jutrzenka Trzebiatowska P, Dzierbicka A, Kamińska N, Datta J. The influence of different glycerine purities on chemical recycling process of polyurethane waste and resulting semi-products. *Polym Int.* 2018;67:1368–77.
25. Kasprzyk P, Benes H, Keitel R, Datta J. The role of hydrogen bonding on tuning hard-soft segments in bio-based thermoplastic poly (ether-urethanes). *J Clean Prod.* 2020;274:122678. <https://doi.org/10.1016/j.jclepro.2020.122678>.
26. Parcheta P, Malka I, Głowińska E, Datta J. Thermal degradation kinetics of poly(propylene succinate) prepared with the use of natural origin monomers. *Polimery.* 2018;63:700–7.
27. Park SH, Oh KW, Kim SH. Reinforcement effect of cellulose nanowhisker on bio-based polyurethane. *Compos Sci Technol.* 2013;86:82–8. <https://doi.org/10.1016/j.compscitech.2013.07.006>.
28. Hatakeyama H, Tanamachi N, Matsumura H, Hirose S, Hatakeyama T. Bio-based polyurethane composite foams with inorganic fillers studied by thermogravimetry. *Thermochim Acta.* 2005;431:155–60.
29. Chattopadhyay DK, Webster DC. Thermal stability and flame retardancy of polyurethanes. *Prog Polym Sci.* 2009;34:1068–133.
30. Mizera K, Ryszkowska J. Thermal properties of polyurethane elastomers from soybean oil-based polyol with a different isocyanate index. *J Elastomers Plast.* 2019;51:157–74.
31. Chuang FS, Tsen WC, Shu YC. The effect of different siloxane chain-extendors on the thermal degradation and stability of segmented polyurethanes. *Polym Degrad Stab.* 2004;84:69–77.
32. Rosu D, Tudorachi N, Rosu L. Investigations on the thermal stability of a MDI based polyurethane elastomer. *J Anal Appl Pyrolysis.* 2010;89:152–8. <https://doi.org/10.1016/j.jaap.2010.07.004>.
33. Lu MG, Lee JY, Shim MJ, Kim SW. Thermal degradation of film cast from aqueous polyurethane dispersions. *J Appl Polym Sci.* 2002;85:2552–8.

**Publisher's Note** Springer Nature remains neutral with regard to jurisdictional claims in published maps and institutional affiliations.